# Broadband dielectric characterization of carbon black reinforced natural rubber

*Menglong Huang,[1] Lewis B. Tunnicliffe,[1] Shibai Liao,[1] Bin Yang,[2] Haixue Yan,[1] James J.C. Busfield [1*]*

[1]School of Engineering and Materials Science, Queen Mary University of London, Mile End Road, London, E1 4NS, UK

[2]School of Electrical Engineering & Computer Science, Queen Mary University of London, Mile End Road, London, E1 4NS, UK

**KEYWORDS**: Natural rubber, carbon black, broadband dielectric spectroscopy, impedance, Terahertz

## ABSTRACT

Natural rubber compounds reinforced with two different carbon blacks (N134 and N330) at various concentrations were characterized using very broadband dielectric spectroscopy from around 0.1 Hz to 0.3 THz using four different impedance and network analysis technologies. Percolation behaviour was observed when the testing electrical frequency is below a certain range, which can be linked to the presence of percolated carbon black networks. When above a critical frequency level, the real part of AC conductivity or the permittivity tends to have a simple exponential relationship with the volume fraction of carbon black, rather than a percolation-like behaviour with the carbon black volume fraction and is no longer sensitive to carbon black networks. The AC conductivity derived via complex impedance is also strongly influenced by the choice of calculation model when the material is around or below the percolation threshold.

## INTRODUCTION

Nanometric particulates such as carbon black (CB) or precipitated silica not only reinforce the mechanical performance of elastomer materials, but also greatly increase the system complexity. This makes material design challenging, as any minor changes in ingredients or processing can have significant and multi-scale impacts on the final product. It also becomes difficult to accurately allocate the root causes of observed material behaviours, such as the well-known nonlinear dynamic mechanical properties (Payne Effect), which remains challenging for constitutive modelling due to the difficulty in accurately decoupling the various microstructural

origins.[1,2] Additionally, traditional material characterization methods typically reflect bulk properties, therefore it is important to employ different testing methods that can sensitively capture one or multiple local behaviours of the reinforced elastomer composites over different length scales.

Broadband dielectric spectroscopy covers a wide frequency range, from millihertz (mHz) to Terahertz (THz), spanning over 15 orders of magnitude. Such broad length scales make it uniquely sensitive for the identification of specific local structures. To achieve such a broadband range, different testing technologies are needed. The impedance measurement is typically realized by auto-balancing bridge technologies, which involves an automated process to maintain circuit balance, facilitating precise measurement of complex impedance elements through constant readjustment. It is amongst the most widely used methods because enormous amounts of information can be derived at a low cost in testing. It typically covers from 1 Hz to 1 Megahertz (MHz) range (6 orders of magnitude), within which the most important segmental relaxation processes of polymer chains can be characterized over a specified temperature range.[3–7] The deconvolution technique applied via Havriliak-Negami (HN)[8] empirical functions makes it possible to decouple different relaxation processes occurring in local phases. However, composites containing conductive particulates such as CBs become conductive when the particulate amount is above a certain level (known as the percolation threshold). Such electrical conductivity significantly contributes to the measured impedance loss especially at low frequency ranges. It may even override other dielectric relaxation processes and potentially creates misleading results. Therefore, it is challenging to discuss dielectric relaxations of materials that exhibit high impedance loss due to the formation of conductive networks[9] in a typical impedance test.

In order to cover broader frequency ranges, it is necessary to couple together a range of different testing techniques besides a typical auto-balancing bridge impedance mentioned above. For example, RF I-V impedance technique[10] can cover the electrical frequency range from MHz up to gigahertz (GHz) with better accuracy compared to the vector network analysis (VNA) method. The vector network analysis is extensively utilized in the gigahertz range. It typically involves transmitting and receiving electromagnetic signals through materials to determine its characteristics such as complex permittivity. There are several ways to connect the material to the VNA testing systems. For example, a typical VNA driven cavity-based microwave characterisation method derives the material electromagnetic property at a single frequency[11]. However, it fits better only for the low dielectric loss materials. Waveguides can also be connected to VNA systems, which can offer wider microwave band characterisation. However, the specimens have to be prepared to exactly fit into the size of waveguide[12]. Due to such set-up requirements, it is almost impossible to apply another stimulus to the material under testing such as an in-situ tensile frame.

As a comparison, the VNA driven free-space millimetre wave measurement system offers much greater flexibility in terms of experimental setup. For example, THz time-domain spectroscopy

(THz-TDS) testing methods[13,14] apply transmission and reflection techniques in order to measure the electromagnetic parameters (such as the complex permittivity) over the millimetre and submillimetre wave range up to 5 THz. It is simple and flexible to setup, as the material under test is held in free space, eliminating the need for additional electrodes or waveguides. As a result, the material can be placed in an oven to enable temperature testing[15] or even temperature scanning to be undertaken. Moreover, a tensile frame could also be implemented in order to study the strain dependent electromagnetic properties[16]. As in other transmission/reflection tests, transmission/reflection coefficients are initially determined using the VNA equipment from which other electromagnetic parameters can be derived[14].

Some of the techniques, especially those for THz range testing, are still relatively new to the rubber industry and are quite expensive. As a result, there have been only a limited number of investigations reporting the full broadband spectrum. For example, Adriaanse et al[17] investigated the percolation behavior of carbon black reinforced thermosets up to THz frequency, discovering that the frequency dependence conductivity behavior can be described well by an extension of the anomalous diffusion model for electron hopping on a fractal. More recently, Okano et al[16,18] studied the broadband spectrum of SBR composites filled by carbon black with a focus on the terahertz time-domain spectroscopy and its strain-dependent behavior. Such free-space techniques can be especially useful when it is necessary to decouple the effects from conductive particle/particle networks. To the best of the authors' knowledge, there have been few studies that have investigated the broadband spectrum of carbon black filled natural rubber (NR) composites, despite its significance in the rubber industry.

This report presents the full broadband spectrum (ranging from 0.1Hz to 0.3 THz) of carbon black-reinforced natural rubber model compounds covered by four different testing techniques. This spectrum provides a comprehensive overview of different relaxation processes, in contrast to a single frequency impedance test that only provides a limited subset of this information. This has relevance for various microwave technology applications, such as electrical sensors, microwave absorption and electromagnetic shielding[19], which require such knowledge of the dielectric behaviour across a wide range of frequencies. Additionally, a detailed analysis of impendence measurement is discussed, showing the importance of the testing frequency and the applied calculation model.

# EXPERIMENTS

## *Materials*

Natural rubber (SMR CV60) and carbon black (N134 or N330) masterbatches having a carbon black volume fraction $\phi$ = 0.204 were prepared by compounding in a Banbury-type internal mixer for 5 min at around 149 °C with a rotor speed of 80 rpm (performed at Cabot Corporation, Boston, MA). According to the ASTM D-1765, the NSA (nitrogen absorption) surface areas of N134 and N330 are 143 and 78 $m^2/g$ respectively. Additionally, the OAN (oil absorption number) structure of N134 and N330 are 127 and 102 $m^2/g$ respectively. When compared at equal volume fraction

in rubber, the smaller primary particle size (higher surface area) of N134 versus N330 results in significantly more particles per unit volume of compound, smaller interparticle gap distance and consequently more particle-particle and particle polymer interactions. The NR/CB Master baches were diluted via a two-roll mill with different amounts of unfilled NR (SMR CV60) to create compounds with a range of carbon black volume fractions. Afterwards, the cure ingredients of 2 phr (parts per hundred grams of rubber) of dicumyl peroxide (Sigma Aldrich, UK) were also introduced into each batch using the mill. Finally, all materials were vulcanized at 160 °C under a pressure of around 60 bar for 1 h, resulting in rubber sheets with a thickness of around 0.7 mm. Fifteen different compounds were used in this study as identified in TABLE 1

*TABLE 1 List of the different material samples used in this paper. (phr: per hundred grams of rubber)*

| Sample Code | Filler Type | Filler Amount [phr] | Filler Volume Fraction $\phi$ |
|---|---|---|---|
| **NR/0** | / | 0 | 0 |
| **N134/0.025** | N134 | 5 | 0.025 |
| **N134/0.049** | N134 | 10 | 0.049 |
| **N134/0.071** | N134 | 15 | 0.071 |
| **N134/0.093** | N134 | 20 | 0.093 |
| **N134/0.133** | N134 | 30 | 0.133 |
| **N134/0.170** | N134 | 40 | 0.170 |
| **N134/0.204** | N134 | 50 | 0.204 |
| **N330/0.025** | N330 | 5 | 0.025 |
| **N330/0.049** | N330 | 10 | 0.049 |
| **N330/0.071** | N330 | 15 | 0.071 |
| **N330/0.093** | N330 | 20 | 0.093 |
| **N330/0.113** | N330 | 25 | 0.113 |
| **N330/0.133** | N330 | 30 | 0.133 |
| **N330/0.152** | N330 | 35 | 0.152 |
| **N330/0.170** | N330 | 40 | 0.170 |
| **N330/0.187** | N330 | 45 | 0.187 |
| **N330/0.204** | N330 | 50 | 0.204 |

### *DC conductivity measurement*

The DC conductivity was measured using a Keithley 6517A electrometer through an unshielded connection. Each sample had dimensions of 20 mm × 20 mm × 0.7 mm. A pair of copper disc electrodes, each with a 14 mm diameter, were employed with the sample inserted between them. A voltage potential was applied across the sample thickness, and the resulting current was measured. Ohm's law was used to calculate the DC resistance, and the DC conductivity was ultimately determined based on the sample's geometry.

*Impedance tests (0.1 Hz to 1GHz)*

Auto-balancing bridge impedance tests were carried out from 0.1 Hz to 1 MHz using a Novocontrol Concept 40 Dielectric Spectrometer at room temperature. Specimen dimensions were 25 mm x 25 mm x 0.7 mm and the surface of each sample was coated by gold using vacuum deposition to ensure a good surface contact with the electrodes (the thickness of gold was around 100 nm). The diameter of the overlapping gold layers was 22 mm allowing the impedance of the specimen sandwiched between the electrodes to be measured. RF I-V Impedance tests were carried out via an Agilent 4291B RF Impedance Spectrometer. The complex permittivity was measured between 100 MHz and 1 GHz at room temperature for all the samples. The test specimens had dimensions around 30 mm x 20 mm x 0.7 mm. The equipment was calibrated using a standard PTFE block sample. All the samples were directly clamped using a standard Agilent 16453A test fixture where a minimum constant clamping force was used.

The impedance instruments deliver the complex impedance $Z^* = R + iX$, where $R$ and $X$ are the real and imaginary part of impedance respectively, by applying a sinusoidal voltage and measuring the resulting sinusoidal current. The material under test is placed between two parallel electrodes, which can be treated as an ideal resistor and an ideal capacitor connected in series or in parallel. Based on this approach, the capacitance can be calculated using either the series or parallel model or even more complicated models. The complex permittivity $\kappa^* = \kappa' - i\kappa''$ can be further worked out, where $\kappa'$ and $\kappa''$ are the real and imaginary part of the permittivity respectively. Accordingly, AC conductivity can also be derived

$$\sigma^*_{ac} = \sigma'_{ac} - i\sigma''_{ac} = i2\pi\kappa_0(\kappa^* - 1) \quad (1)$$

where $\sigma'_{ac}$ and $\sigma''_{ac}$ are the real and imaginary components of the AC conductivity respectively. $\kappa_0$ is the permittivity of the free space. Therefore, the $\kappa^*$ and $\sigma^*_{ac}$ value depends on the model chosen. For example, by applying a series or a parallel model, $\sigma'_{ac}$ can be derived as

$$\sigma'_{ac,\,series} = \frac{t \cdot R}{s \cdot X^2} \quad (2)$$

or

$$\sigma'_{ac,\,parallel} = \frac{t \cdot R}{s \cdot (X^2 + R^2)} \quad (3)$$

respectively, where $t$ is the material thickness and $s$ is the area. It can be seen that the absolute $\sigma'_{ac}$ value can be highly dependent on the applied mode. Throughout this article, series models are applied unless it is indicated separately.

*Microwave test (7-40 GHz)*

Microwave characterisation was used to measure the complex permittivity of all the samples at six different frequencies: 7, 9, 11, 25, 30 and 40 GHz at room temperature. The transmission and reflection parameters were obtained using a Wiltron 37269A Network Analyser. The sample size (length and width) varied depending upon the size of the wave guide used. For 7, 9 and 11 GHz testing: the rubber specimens were cut into a dimension of 22.86 mm × 10.16 mm. While 7.11 mm × 3.56 mm was used to test the remaining frequencies. The thickness of all samples was

around 0.7 mm. The complex permittivity was derived from the measured transmission and reflection parameters[20,21].

*THz time-domain spectroscopy (0.2-0.3 THz)*

Millimetre wave transmission measurements were performed via an HP N5244A vector network analyser and its millimetre wave extension heads. As shown in Figure 1(a), the testing signal transports from the transmitter to receiver via four reflectors while the material is held between Reflector 2 and Reflector 3.[22] Figure 1(b) shows an enlarged view of the area where the sample is held. The transmission and reflection parameters were recorded and the complex permittivity was obtained via non-linear fitting techniques using transmission functions[23,24]. At an instance, VNA measures reflection and transmission coefficients (S11 and S21), which can be described as:

$$S_{11} = \frac{\Gamma(1-T^2)}{1-\Gamma^2T^2} \quad (4)$$

$$S_{21} = \frac{T(1-\Gamma^2)}{1-\Gamma^2T^2} \quad (5)$$

where Γ is the reflection coefficient while $T$ is the transmission coefficient. They both can be explained by the wave propagation constant $\gamma$ and the complex wave impedance $Z_{sn}$:

$$\Gamma = \frac{Z_{sn}-1}{Z_{sn}+1} \quad (6)$$

$$T = e^{-\gamma d} \quad (7)$$

where $\gamma$ and $Z_{sn}$ can be further explained by the complex permittivity ($\kappa^*$) and complex permeability ($\mu^*$) of the material:

$$\gamma = \gamma_0\sqrt{\kappa^*\mu^*} \quad (8)$$

$$Z_{sn} = \sqrt{\mu^*/\kappa^*} \quad (9)$$

where $\mu^*$ = 1 for non-magnetic materials such as the rubber composites used in this study.

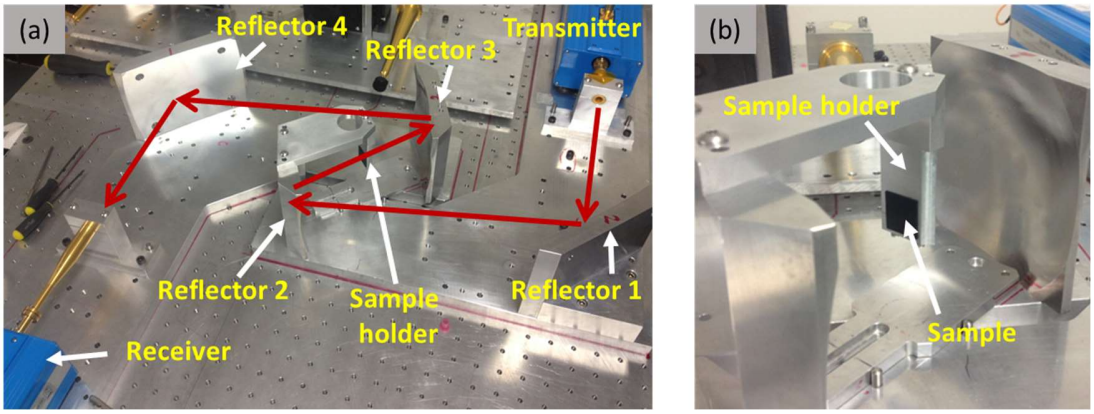


*Figure 1 (a) The setup of a quasi-optical dielectric testing system (transmission). (b) A close up of the sample holder shown in (a).*

# RESULT AND DISCUSSION

## *Impedance and AC conductivity*

As explored in the experimental section, impedance tests yield complex impedance values, while other electrical parameters like capacitance, permittivity, and AC conductivity must be calculated using suitable models. These models can range from a simple resistor connected in series or parallel with a capacitor to more complex configurations involving hundreds or even thousands of elements linked randomly[25]. Although models can play a significant role in understanding the calculated results, however, they have rarely been discussed by the composite community. Figure 2(a) illustrates the model dependency of $\sigma'_{\mathrm{ac}}$, which is also highly influenced by testing frequency and $\phi$. When $\phi$ is small (N330/0.049), $\sigma'_{\mathrm{ac,\,series}}$ and $\sigma'_{\mathrm{ac,\,parallel}}$ exhibit a difference of roughly five orders of magnitude across the entire frequency range. Adding more carbon black (N330/0.170), reduces such difference at low frequency ranges, such as below 10 Hz. When sufficient carbon black is incorporated into the system, the model's impact diminishes or even disappears across all frequencies (N330/0.204). This model dependency inversely corresponds to the measured impedance loss

$$D = \frac{X}{R} = D_{dc} + D_{dipoles} \tag{10}$$

where $D_{dc}$ represents the loss from DC conductivity and $D_{dipoles}$ accounts for the dielectric loss from various types of dipoles.[9] In carbon black filled composites, $D$ is driven by $D_{dc}$ especially at low frequencies like below 100 Hz. In summary, the model dependency of $\sigma'_{\mathrm{ac}}$ intensifies when the material has a smaller $\sigma_{\mathrm{dc}}$ and is measured at lower frequency ranges.

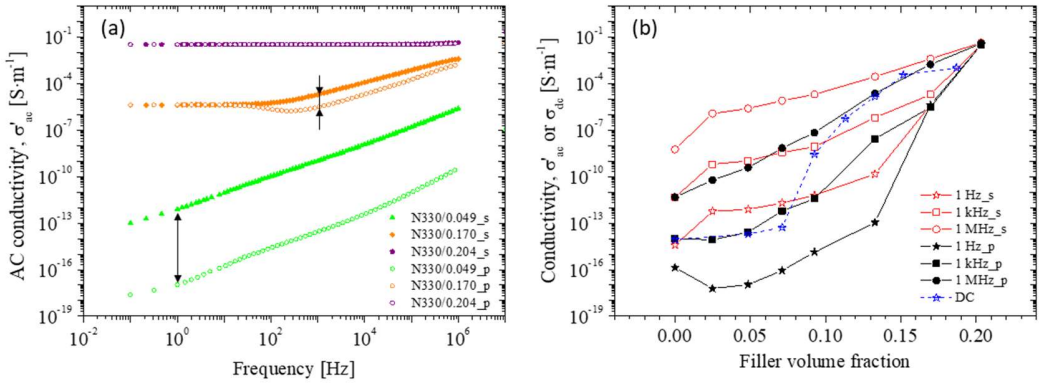


*Figure 2 (a) Frequency dependency of AC conductivity derived via either series or parallel model for samples filled by N330. They are marked as "_s" or "_p" respectively. (b) The filler volume fraction dependency of AC or DC conductivity. AC conductivity derived via either series or parallel model at different frequencies.*

Figure 2(b) displays the DC conductivity percolation threshold $\phi_c^{dc}$ (where $\sigma_{\mathrm{dc}}$ experiences a sudden order of magnitude change) at approximately $\phi$ =0.093, differing from the AC conductivity percolation threshold $\phi_c^{ac}$ shown in the same plot. Moreover, $\phi_c^{ac}$ itself is also frequency and model dependent. By definition, $\sigma'_{\mathrm{ac}}$ should generally be greater than $\sigma_{\mathrm{dc}}$ at all

frequencies, with both values converging as the frequency approaches zero. However, in Figure 2(b), $\sigma_{dc}$ is larger than $\sigma'_{ac}$ (1Hz, parallel model) for all samples except the most conductive N330/0.204. Even in a series model characterized at 1 Hz: N330/0.093, N330/0.133, and N330/0.170 samples exhibit lower $\sigma'_{ac}$ than $\sigma_{dc}$. This discrepancy may arise from several factors: First, the testing conditions differ significantly: $\sigma_{dc}$ is characterized at very high voltages exceeding 100 volts for less conductive materials, while the impedance test utilizes a 1-volt signal in order to minimize side effects from the applied electric field. It is a common observation that composites filled with conductive or semiconductive fillers may exhibit non-linear current-voltage (I-V) characteristics.[26] Second, the local-scale heterogeneity of rubber composites significantly increases system complexity. A single Resistance-Capacitance model might cause a noticeable offset in the calculated results, particularly for materials around the percolation region. Third, the electrical and dielectric properties of rubber compositions are highly sensitive to applied deformation and deformation history, even when attempts are made to minimize deformation histories.[9,27] Such deformations typically result in a substantial decrease in $\sigma'_{ac}$ and $\kappa'$ due to the breakdown of "particle-particle" networks beginning at strains as small as 0.1% or even less.[9] During sample preparation, vacuum coating, and testing, it is nearly impossible to avoid material deformation. Consequently, the measured $\sigma'_{ac}$ is likely to be lower than anticipated. This testing challenge also arises in other elastomer evaluations, such as dynamic mechanical analysis (DMA).

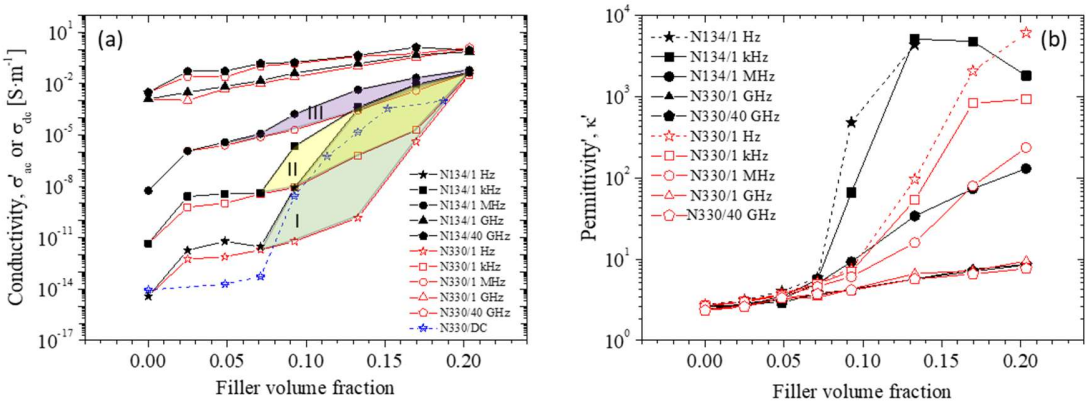


*Figure 3 The real part of AC conductivity (a) and permittivity (b) at the selected frequencies.*

As discussed above, $\sigma_{dc}$ plays a crucial role in determining $\sigma'_{ac}$ and $D$. It is well-established that $\sigma_{dc}$ is proportional to the amount of percolated carbon black networks within the rubber compound. N134 carbon black generates more networks in a compound than N330 due to its higher surface area and structure, resulting in a higher $\sigma'_{ac}$ for N134-filled compounds compared to those filled with N330, as seen in Figure 3(a). However, as the electrical frequencies increase, the impact of $\sigma_{dc}$ or carbon black networks on $\sigma'_{ac}$ diminishes. For instance, zones I, II, and III in Figure 3(a) clearly demonstrate that the difference in $\sigma'_{ac}$ between N330 and N134 filled compounds narrows with increasing testing frequency. In other words, the contribution from

active particle-particle networks decreases with increasing frequency. When the electrical frequency is high enough, such as above 1 GHz, log($\sigma'_{\mathrm{ac}}$) exhibits a direct relationship with filler volume fraction, regardless of filler type. This trend has also been reported in carbon black-reinforced thermosets.[17] The same trend is observed *for* $\kappa'$ in Figure 3(b)*,* suggesting that dipole-related particle networks and particle-particle interfaces are no longer active at high frequencies. Such inactivity occurs because the length scale of carbon black networks is too large to be detected in such high-frequency domains. Consequently, it is advisable to use low frequencies, such as 1 Hz, to study the percolation behaviour of $\kappa'$ and $\sigma'_{\mathrm{ac}}$.

### *Broadband spectrum*

Figure 4 presents the full broadband dielectric spectrum of samples reinforced by carbon black N134 and N330. Although these graphs are built from a combination of different testing techniques, they appear to show a good level of internal consistency between the various different test frequency regimes. In Figure 4 (a), $\kappa'$ increases as with the increase of $\phi$, except for the highest carbon black volume fractions such as N134/0.170 and N134/0.204. The drop in $\kappa'$ at low frequencies for these samples results from the testing equipment limitations, as the impedance loss in these cases is very high due to the elevated $D_{dc}$. As previously noted in the literature, these data points can be disregarded.[28] It is also important to note that in cases where $\kappa'$ is particularly high, such as when it exceeds 100 as shown for some specimens with higher $\phi$ in Figure 4(a) and (b), the value may not reflect the intrinsic permittivity of the composite materials. Instead, it could be a result of testing and interpolation based on measured complex impedance.[29]

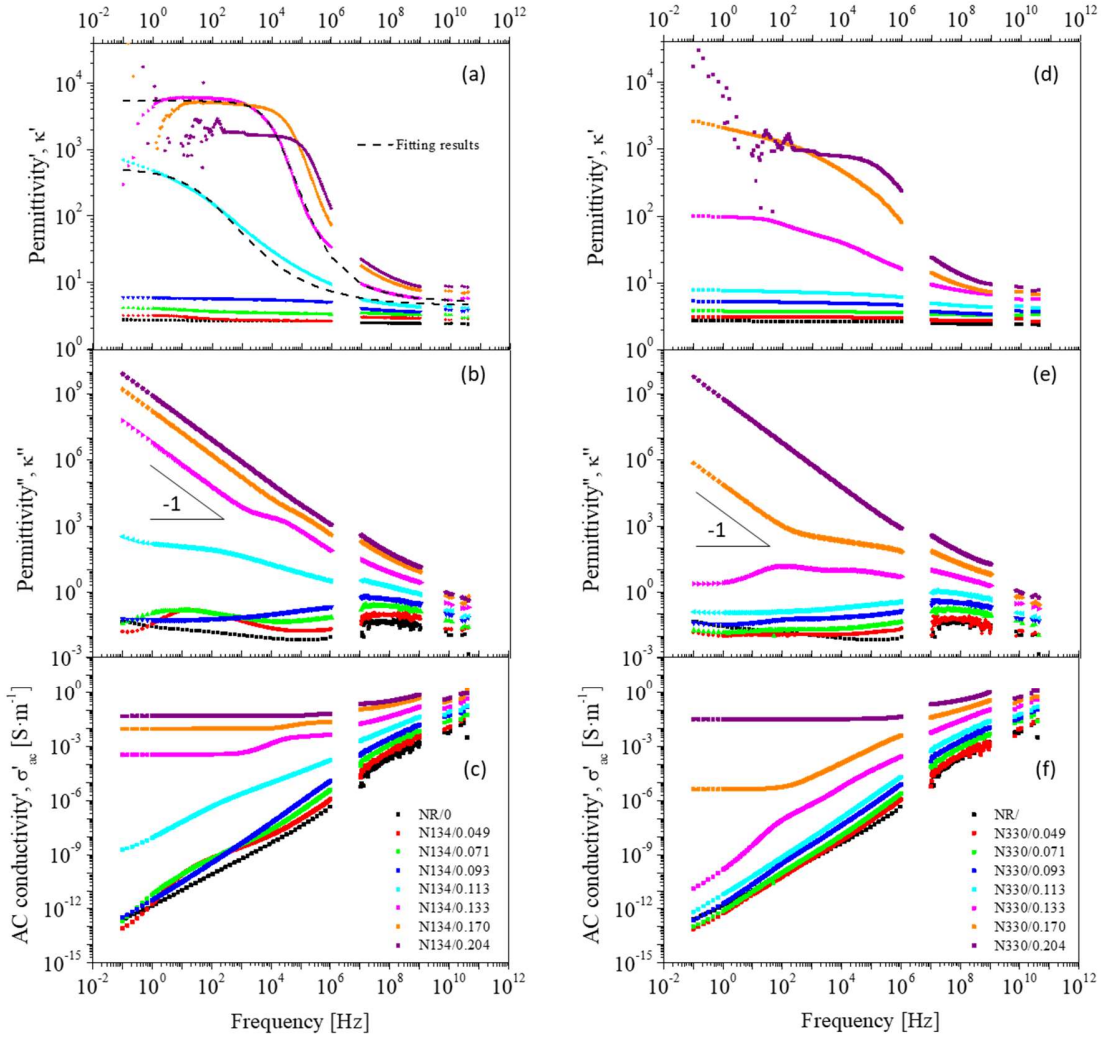


*Figure 4. The frequency dependent dielectric behaviour of carbon black N134 (a, b & c) and N330 (d, e & f) filled natural rubber presented by the real and imaginary part of permittivity as well as the real part of the ac conductivity. Symbols shown in (c) and (f) are the same for the rest of the graphs.*

Both Figure 4 (a) and (d), show a step decrease in $\kappa'$ for highly loaded samples, similar to a typical dipole relaxation process[30], although lacking a corresponding $\kappa''$ peak at the respective frequencies. Considering the frequency domain processes in Figure 4(a) and (b) caused by dipole relaxations, the data can be fitted via Havriliak-Negami (HN)[8] empirical functions. However, although single fitting of $\kappa'$ is possible using HN functions, simultaneously satisfying the fitting of both $\kappa'$ and $\kappa''$ is very challenging. Two example fittings are shown in Figure 4(a). Furthermore, as mentioned earlier, $\kappa^*$ derived from impedance tests is model-dependent. Unlike $\sigma'_{ac}$ (Figure 2), $\kappa^*$ exhibits strong model dependency when D>0.1. Therefore, discussing dielectric relaxation processes for composites with significant impedance loss is not recommended. The colossal $\kappa'$ measured by the impedance method for conductive composites can no longer be explained solely by dipole relaxation processes but is dominated by testing, calculation and $\sigma_{dc}$.

However, this misunderstanding of such 'dielectric' phenomena has existed since 1980s in the composite community. In 1982, Kawamoto[31] observed a dramatic decrease of permittivity at around 100 Hz for his carbon black (CB) filled rubbers which he treated as a relaxation. He explained this relaxation as resistor-capacitor (RC) resonance where the gaps between particles can be treated as a resistor in parallel with a capacitor. Following this idea, Ouyang[32] and Geberth[33] used Havriliak-Negami (HN)[8] type functions to fit the frequency dependent $\kappa'$ test results and obtained a so-called relaxation time. Moreover, they applied tunnel conducting mechanism into Kawamoto's RC model and obtained an average distance between particles. This approach has also been cited by other studies.[34] More recently, Nuzhnyy[28] attempted simultaneous fitting of both $\kappa'$ and $\kappa''$ of MWCNT/PC composites. Although $\kappa'$ fitted their results well, $\kappa''$ was less well fitted. They had to adopt multiple relaxation processes with 14 different fitting parameters to balance the results without concrete underlying physical model. Although single $\kappa'$ fitting is not reliable, single fitting of $\kappa''$ seems more widely accepted[30] as it reveals different peaks related to various relaxation processes. When $\phi$ approaches $\phi_c^{dc}$, $\kappa''$ exhibits a slope of -1 versus the electrical frequency when the frequency is low enough, as shown in Figure 4 (b) and (e). Simultaneously, the $\sigma'_{\mathrm{ac}}$ shows a plateau in the corresponding area as depicted in Figure 4 (c) and (f).

### *Terahertz Spectroscopy*

Figure 5 presents the results of the THz spectra of N330-filled samples obtained through the transmission mode. Figure 5(a) shows that $\kappa'$ remains stable in the tested frequency range for N330-filled rubber up to 40 phr (N330/0.170). However, when $\phi \geq 0.093$ (20 phr), the spectrum appears much more erratic of $\kappa''$ as shown in Figure 5(b). This may be due to the contribution from the DC conductivity network from carbon blacks, which leads to a certain level of instability in the transmission tests. These fitting results could potentially be improved if a DC conductivity term were included during fitting. Nevertheless, the carbon black network should not significantly contribute to an increase in $\kappa'$ at such high frequency ranges, while the volume fraction of carbon black plays a more substantial role. This is indirectly supported by the results in Figure 3(*b*), which show that the type of carbon black has limited impact on $\kappa'$ when the frequency is above 1 GHz, despite N134 having distinct surface features and increased particle-particle contacts within the NR matrix when compared to N330.[35] It is worth noting that the strain-dependent dielectric behaviour in the terahertz range observed by Mizuta et al[16] could also be attributed to sub-effects from tensile deformation rather than the DC conductivity networks.

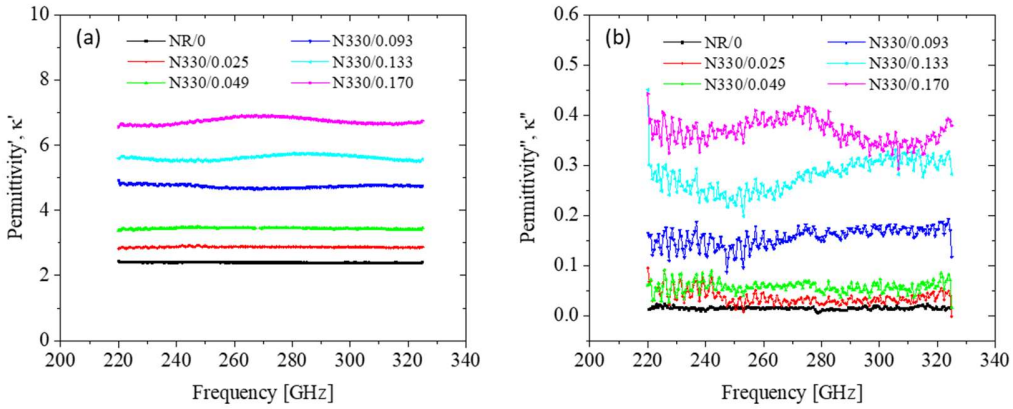


*Figure 5 THz spectrum of compounds filled by N330 carbon black.*

## Conclusion

A broadband dielectric spectrum of the natural rubber/carbon black system has been constructed via different testing methods. In an impedance test, the complex permittivity and AC conductivity are highly dependent on the testing frequency and calculation models applied for NR/CB compounds or composites reinforced by conductive fillers. One has to be very careful when making use of the results from the impedance tests for those types of materials. When at low frequencies such as 1 Hz, the carbon black networks dominate the measured results, while at high frequency like 1 GHz, the dielectric property of materials is not sensitive to particle networks anymore. For example, the $\log(\sigma'_{ac})$ shows a linear relationship to the carbon black volume fraction irrespective of the carbon black type. Therefore, the high frequency dielectric test offers a chance to decouple the impact of the carbon black networks from other features of a rubber compound.

## ACKNOWLEDGMENTS

The authors would like to thank Professor Alan G. Thomas from Queen Mary University of London for his continuous support on our investigation into broadband dielectric spectroscopy of carbon black filled elastomer composites. The QMUL team will be forever indebted for his wonderful insights in completing this and many other investigations into the behaviour of rubber. M.H. would like to thank the China Scholarship Council for doctoral funding and Cabot Corporation (Boston, USA) for kindly providing the materials. The authors would like to thank Professor Jiaming Tang and Dr Gang Zhao from Xidian University in China for helping with the microwave characterization. The authors would also like to thank Dr Jian Zhuang and Professor Xiaoyong Wei from Xi'an Jiaotong University for discussions concerning the design of the test.

## PRESENT ADDRESS

M.H.: Continental Reifen Deutschland GmbH, Jaedekamp 30, 30419 Hannover, Germany.

L.B.T.: Birla Carbon, 1800 West Oak Commons Court, Marietta, GA 30062, US.
S.L.: Henkel (China) Investment Co., Ltd. 99 Jiang Wan Cheng Road, Shanghai, 200438, China.
B.Y.: Faculty of Science and Engineering, University of Chester, Parkgate Road, CH1 4BJ, UK.

## REFERENCES

(1) Fletcher, W. P.; Gent, A. N. Nonlinearity in the Dynamic Properties of Vulcanized Rubber Compounds. *Rubber Chem. Technol.* **1954**, *27* (1), 209–222.
(2) Payne, A. R. The Dynamic Properties of Carbon Black Loaded Natural Rubber Vulcanizates. Part II. *J. Appl. Polym. Sci.* **1962**, *6* (21), 368–372.
(3) Ngai, K. L.; Plazek, D. J. Identification of Different Modes of Molecular Motion in Polymers That Cause Thermorheological Complexity. *Rubber Chem. Technol.* **1995**, *68* (3), 376–434.
(4) Robertson, C. G.; Roland, C. M. Glass Transition and Interfacial Segmental Dynamics in Polymer-Particle Composites. *Rubber Chem. Technol.* **2008**, *81* (3), 506–522.
(5) Roland, C. M. ELECTRICAL AND DIELECTRIC PROPERTIES OF RUBBER. *Rubber Chem. Technol.* **2015**.
(6) Huang, M.; Tunnicliffe, L. B.; Thomas, A. G.; Busfield, J. J. C. The Glass Transition, Segmental Relaxations and Viscoelastic Behaviour of Particulate-Reinforced Natural Rubber. *Eur. Polym. J.* **2015**, *67* (0), 232–241.
(7) Lindemann, N.; Finger, S.; Karimi-Varzaneh, H. A.; Lacayo-Pineda, J. Rigidity of Plasticizers and Their Miscibility in Silica‐filled Polybutadiene Rubber by Broadband Dielectric Spectroscopy. *J. Appl. Polym. Sci.* **2022**, *139* (21), 52215.
(8) Havriliak, S.; Negami, S. A Complex Plane Representation of Dielectric and Mechanical Relaxation Processes in Some Polymers. *Polymer* **1967**, *8*, 161–210.
(9) Huang, M.; Tunnicliffe, L. B.; Zhuang, J.; Ren, W.; Yan, H.; Busfield, J. J. C. Strain-Dependent Dielectric Behavior of Carbon Black Reinforced Natural Rubber. *Macromolecules* **2016**.
(10) Okada, K.; Sekino, T. Impedance Measurement Handbook. *Agilent Technologies* **2003**, *128*, 5950–3000.
(11) Zhang, M.; Tang, Z.; Zhang, H.; Smith, G.; Jiang, Q.; Saunders, T.; Yang, B.; Yan, H. Characterization of Microwave and Terahertz Dielectric Properties of Single Crystal La2Ti2O7 along One Single Direction. *J. Eur. Ceram. Soc.* **2021**, *41* (14), 7375–7379.
(12) Al-Moayed, N. N.; Afsar, M. N.; Khan, U. A.; McCooey, S.; Obol, M. Nano Ferrites Microwave Complex Permeability and Permittivity Measurements by T/R Technique in Waveguide. *IEEE Trans. Magn.* **2008**, *44* (7), 1768–1772.
(13) Donnan, R. S.; Martin, D. H.; Wylde, R. J.; Yang, B. *Assessment of Magnetic Materials for Use in Quasi-Optical Non-Reciprocal Devices Operating at Frequencies above 90 GHz*; Infrared and Millimeter Waves, 2007 and the 2007 15th International Conference on Terahertz Electronics. IRMMW-THz. Joint 32nd International Conference on; IEEE, 2007.
(14) Wu, B.; Tuncer, H. M.; Naeem, M.; Yang, B.; Cole, M. T.; Milne, W. I.; Hao, Y. Experimental Demonstration of a Transparent Graphene Millimetre Wave Absorber with 28% Fractional Bandwidth at 140 GHz. *Sci. Rep.* **2014**, *4*.

(15) Varadan, V. V.; Hollinger, R. D.; Ghodgaonkar, D. K.; Varadan, V. K. Free-Space, Broadband Measurements of High-Temperature, Complex Dielectric Properties at Microwave Frequencies. *IEEE Trans. Instrum. Meas.* **1991**, *40* (5), 842–846.
(16) Mizuta, K.; Okano, M.; Morimoto, T.; Ata, S.; Watanabe, S. Strain-Induced Irreversible Change of the Conductive Network in a Rubber/Carbon-Black Composite Revealed by Polarization-Resolved Terahertz Dielectric Spectroscopy. *Appl. Phys. Lett.* **2022**, *121* (2), 024101.
(17) Adriaanse, L. J.; Reedijk, J. A.; Teunissen, P. A. A.; Brom, H. B.; Michels, M. A. J.; Brokken-Zijp, J. C. M. High-Dilution Carbon-Black/Polymer Composites: Hierarchical Percolating Network Derived from Hz to THz Ac Conductivity. *Phys. Rev. Lett.* **1997**, *78* (9), 1755.
(18) Okano, M.; Watanabe, S. Internal Status of Visibly Opaque Black Rubbers Investigated by Terahertz Polarization Spectroscopy: Fundamentals and Applications. *Polymers* **2018**, *11* (1). https://doi.org/10.3390/polym11010009.
(19) Al-Saleh, M. H.; Saadeh, W. H.; Sundararaj, U. EMI Shielding Effectiveness of Carbon Based Nanostructured Polymeric Materials: A Comparative Study. *Carbon N. Y.* **2013**, *60*, 146–156.
(20) Zhao, F.; Sha, C. T.; Zhao, G.; Wang, K.; Kan, J. S. *A One-Port Waveguide Method and Its Application in Characterization of Radar Absorbing Materials*; Applied Mechanics and Materials; Trans Tech Publ, 2014; Vol. 496.
(21) Baker-Jarvis, J.; Vanzura, E. J.; Kissick, W. Improved Technique for Determining Complex Permittivity with the Transmission/Reflection Method. *IEEE Trans. Microw. Theory Tech.* **1990**, *38* (8), 1096–1103.
(22) Huang, M. The Strain Dependent Dielectric Behaviour of Carbon Black Filled Natural Rubber. **2016**.
(23) *Experimental Characterization of Hexaferrite Ceramics from 100 GHz to 1THz Using Vector Network Analysis and THz-Time Domain Spectroscopy*.
(24) Yang, B.; Wylde, R. J.; Martin, D. H.; Goy, P.; Donnan, R. S.; Caroopen, S. Determination of the Gyrotropic Characteristics of Hexaferrite Ceramics from 75 to 600 GHz. *IEEE Trans. Microw. Theory Tech.* **2010**, *58* (12), 3587–3597.
(25) Almond, D. P.; Bowen, C. R. Anomalous Power Law Dispersions in Ac Conductivity and Permittivity Shown to Be Characteristics of Microstructural Electrical Networks. *Phys. Rev. Lett.* **2004**, *92* (15), 157601.
(26) Wang, J.; Yu, S.; Luo, S.; Chu, B.; Sun, R.; Wong, C.-P. Investigation of Nonlinear I–V Behavior of CNTs Filled Polymer Composites. *Mater. Sci. Eng. B* **2016**, *206*, 55–60.
(27) Yamaguchi, K.; Busfield, J. J. C.; Thomas, A. G. Electrical and Mechanical Behavior of Filled Elastomers. I. The Effect of Strain. *J. Polym. Sci. B Polym. Phys.* **2003**, *41* (17), 2079–2089.
(28) Nuzhnyy, D.; Savinov, M.; Bovtun, V.; Kempa, M.; Petzelt, J.; Mayoral, B.; McNally, T. Broad-Band Conductivity and Dielectric Spectroscopy of Composites of Multiwalled Carbon Nanotubes and Poly (Ethylene Terephthalate) around Their Low Percolation Threshold. *Nanotechnology* **2013**, *24* (5), 055707.
(29) Lunkenheimer, P.; Bobnar, V.; Pronin, A. V.; Ritus, A. I.; Volkov, A. A.; Loidl, A. Origin of Apparent Colossal Dielectric Constants. *Phys. Rev. B: Condens. Matter Mater. Phys.* **2002**, *66* (5), 052105.
(30) Kremer, F.; Schönhals, A. *Broadband Dielectric Spectroscopy*; Springer: Berlin, 2003.

(31) Sichel, E. K. *Carbon Black-Polymer Composites: The Physics of Electrically Conducting Composites*; Marcel Dekker, Inc: New York, 1982.
(32) Ouyang, G. B. On Immittance Spectroscopy for Carbon Black Network Characterization. *Kautschuk Gummi Kunststoffe* **2002**, *55* (3), 104–113.
(33) Geberth, E.; Klüppel, M. Effect of Carbon Black Deactivation on the Mechanical and Electrical Properties of Elastomers. *Macromol. Mater. Eng.* **2012**, *297* (9), 914–922.
(34) Meier, J. G.; Klüppel, M. Carbon Black Networking in Elastomers Monitored by Dynamic Mechanical and Dielectric Spectroscopy. *Macromol. Mater. Eng.* **2008**, *293* (1), 12–38.
(35) Tunnicliffe, L. B.; Kadlcak, J.; Morris, M. D.; Shi, Y.; Thomas, A. G.; Busfield, J. J. C. Flocculation and Viscoelastic Behaviour in Carbon Black-Filled Natural Rubber. *Macromol. Mater. Eng.* **2014**, *299* (12), 1474–1483.